

The identification of parameters for visco-plastic models via finite-element methods and gradient methods

Rolf Mahnken and Erwin Stein

Institut für Baumechnik und Numerische Mechanik, University of Hannover, Appelstrasse 9a, 30167 Hannover, Germany

Received 4 November 1993, accepted for publication 4 November 1993

Abstract. In this work we present a unified strategy for identification of material parameters of visco-plastic models from test data of complex structures. For consideration of the associated inhomogeneous deformations and stresses the finite-element method is used. The objective function of least-squares type is minimized by a method based on gradient evaluations, such as an SQP method or a projection algorithm due to Bertsekas. The sensitivity analysis, i.e. the determination of the gradient of the objective function, is explained in detail. As a result a recursion formula is obtained. In the numerical examples we compare gradient-based methods with evolutionary methods for homogeneous problems. Concerning inhomogeneous problems we discuss the results obtained for a material law due to Steck.

1. Introduction

The development of material laws for modelling of elasto/visco-plastic deformations consists of both the development of a mathematical model and the determination of material-dependent constants. The identification of these parameters from experimental data requires the solution of inverse problems. So far only uniaxial experiments (see e.g. [7]) have been considered for this task, i.e. field equations have not been taken into account. For minimization of the corresponding objective function stochastic methods such as the evolution strategy [14] are usual. These methods can easily be implemented; however, in general they lead to a long CPU time because of the large number of function evaluations (several 100 000).

The approach in our paper is twofold. Firstly, complex structures such as a plate with a hole are taken into account for determination of the material parameters. Thus plastic and visco-plastic features including hardening are activated by deviatoric stresses. Only in this way is a general verification or falsification of a material law possible. The incorporation of inhomogeneous stresses and strains requires the solution of field equations. For this task the finite-element method (FEM) is used. For time integration of the evolution equations we use the second-order mid-point rule.

Secondly, for minimization of the objective function of least-squares type a method based on gradient evaluations is applied. The specific algorithms are an SQP method [13] or, alternatively, a projection algorithm due to Bertsekas [2]. In order to determine the gradient of the objective function a sensitivity analysis has to be carried out.

2. Formulation of the direct and inverse problems

Let \mathbb{R}^3 be the Euclidean space, and let $\mathcal{I} = [0, T]$ be the time interval of interest. The object of our investigation is a body \mathcal{B} . Let $\Omega \subset \mathbb{R}^3$ be the reference placement of \mathcal{B} with smooth boundary $\partial\Omega$, then any material point $P \in \mathcal{B}$ is defined by $x(P) \in \Omega$. The static equilibrium equation is given by

$$\operatorname{div} \sigma_t + \rho \bar{b} = \mathbf{0} \quad t \in \mathcal{I}, \quad x \in \Omega \tag{1}$$

where σ_t denotes the symmetric Cauchy stress tensor, and $\rho \bar{b}$ is the body force (e.g. the gravity force). As usual we assume

$$\partial\Omega_u \cup \partial\Omega_\sigma = \partial\Omega \quad \partial\Omega_u \cap \partial\Omega_\sigma = \emptyset. \tag{2}$$

We shall denote by \bar{u}_t the prescribed boundary displacement on $\partial\Omega_u$ and designate by \bar{t}_t the prescribed boundary traction vector on $\partial\Omega_\sigma$. In a geometric linear theory with small strains the total strains ε_t can be derived from the displacement u_t according to

$$\varepsilon_t = 1/2 \left((\operatorname{grad} u_t)^T + \operatorname{grad} u_t \right) \tag{3}$$

and we assume an additive split

$$\varepsilon_t = \varepsilon_t^{\text{el}} + \varepsilon_t^{\text{in}}. \tag{4}$$

The elastic part is given by

$$\varepsilon_t^{\text{el}} = \mathbf{C}^{-1} \sigma_t \tag{5}$$

where

$$\mathbf{C} = 2\mu \mathbf{1} + \lambda \mathbf{1} \otimes \mathbf{1} \tag{6}$$

is the elasticity tensor with the Lamé constants μ and λ . Observe that the preceding equations are linear. The source of non-linearity in our problem arises from the type of constitutive equation that relates the stress field and the displacement field as discussed below.

The inelastic part in equation (4) results from the set of evolution equations

$$\dot{\varepsilon}_t^{\text{in}} = f(\kappa, \sigma_t, q_t, t, \dots) \tag{7}$$

$$\dot{q}_t = g(\kappa, \sigma_t, q_t, t, \dots) \tag{8}$$

where q_t are so-called internal variables and $\kappa \in \mathbb{R}^m$ is a vector of m material parameters. It follows that both \mathbf{C} and $\varepsilon_t^{\text{in}}$, q_t are functions dependent on material parameters $\kappa = [\kappa_1, \dots, \kappa_m]^T$.

As an example of a material law the stochastic model due to Steck with seven material parameters and one internal variable is given according to [7, 16]

$$\dot{\varepsilon}_t^{\text{in}} = \frac{3}{2} \dot{\varepsilon}_t^{\text{in}} n_t \tag{9}$$

$$\dot{\varepsilon}_t^{\text{in}} = \lambda' c_1 \exp \left[- \left(1 - \frac{\alpha - 1}{\kappa} \frac{U_0}{RT} \right) \right] \left(2 \sinh \left(\frac{\Delta V}{RT} \sigma_{v,t} \right) \right)^{1+1/\kappa} \exp \left(- \frac{F_t}{RT} \right) \tag{10}$$

$$\dot{F}_t = \frac{1}{\lambda'} \dot{\varepsilon}_t^{\text{in}} - c_2 \exp \left[- \frac{\alpha U_0 - \beta F_t}{RT} \right] \tag{11}$$

$$n_t = \frac{1}{\sigma_{v,t}} s_t \tag{12}$$

$$\sigma_{v,t} = \sqrt{\frac{3}{2} s_t \cdot s_t} \tag{13}$$

$$s_t = \left(\mathbf{1} - \frac{1}{3} \mathbf{1} \otimes \mathbf{1} \right) \sigma_t \tag{14}$$

where $\lambda', \Delta V, c_1, c_2, \alpha, \beta, \kappa$ are material parameters, R is a gas constant and F_t is an internal variable for isotropic hardening.

For complete description of the initial boundary-value problem we assume the initial conditions

$$\mathbf{u}(t = 0) = \mathbf{u}_0 \quad \mathbf{q}(t = 0) = \mathbf{q}_0 \quad \boldsymbol{\sigma}(t = 0) = \boldsymbol{\sigma}_0. \quad (15)$$

Let \mathcal{Y} be the parameter space, and let $\mathcal{U} \times \mathcal{I}$ be the solution space for the displacements of the above initial boundary-value problem. Thus, for a specific set of parameters $\boldsymbol{\kappa} \in \mathcal{Y}$, it is possible to solve the corresponding *direct problem*

$$\boldsymbol{\kappa} \mapsto \mathbf{u}_t(\boldsymbol{\kappa}) \quad (16)$$

in a *forward calculation*. In introducing a solution operator, the corresponding surjective mapping is denoted by

$$S: \begin{cases} \boldsymbol{\kappa} \mapsto \mathbf{u}_t(\boldsymbol{\kappa}) \\ \mathcal{Y} \longrightarrow \mathcal{U} \times \mathcal{I}. \end{cases} \quad (17)$$

Let $\bar{\mathbf{u}}_t \in \mathcal{P} \times \mathcal{I}$ denote given data e.g. from experiments. Then, in general, it is not possible to solve the *inverse problem*

$$\text{find } \boldsymbol{\kappa} : \mathbf{u}_t(\boldsymbol{\kappa}) = \bar{\mathbf{u}}_t \text{ for given } \bar{\mathbf{u}}_t \in \mathcal{P} \times \mathcal{I} \quad (18)$$

in a *backward calculation*. Basically, there are two reasons:

1. In general $\mathcal{U} \times \mathcal{I} \neq \mathcal{P} \times \mathcal{I}$, i.e. the data space cannot be 'reached' by S .
2. There exists no unique operator S^{-1} of S .

Problems of this kind are called *ill posed* problems or *Hadamard* problems (see e.g. [6, 9]). Therefore the backward calculation is replaced by an *optimal approach strategy*, where the solution vector $\mathbf{u}_t(\boldsymbol{\kappa})$ should be as close as possible to the given data $\bar{\mathbf{u}}_t$ in a certain sense. This requirement is expressed by the optimization functional

$$f(\boldsymbol{\kappa}) := \|\mathbf{u}_t(\boldsymbol{\kappa}) - \bar{\mathbf{u}}_t\|_{\mathcal{U} \times \mathcal{I}} \longrightarrow \min_{\boldsymbol{\kappa} \in \mathcal{Y}}. \quad (19)$$

Here, the specific weighted norm on $\mathcal{U} \times \mathcal{I}$ has to be chosen. For instance, in order to take into account the dispersion of measurements, one can implement a dispersity function as a weighting function. Taking an $\|\cdot\|_{L_2}$ -norm (without weighting) leads to the least-squares functional

$$f(\boldsymbol{\kappa}) = \int_0^T \int_{\Omega} (\mathbf{u}_t(\boldsymbol{\kappa}) - \bar{\mathbf{u}}_t)^2 dx dt \longrightarrow \min_{\boldsymbol{\kappa} \in \mathcal{Y}}. \quad (20)$$

Such problems are characterized by the non-convexity of the objective function f and improper conditioning of the Hessian of $f(\boldsymbol{\kappa})$.

3. Solution of the direct problem

3.1. Discrete formulation and solution strategy

For solution of the time-dependent direct problem (16) the balance law (1) is multiplied with test functions $\boldsymbol{\eta}$ of an appropriate Hilbert space

$$\mathcal{V} := \left\{ \boldsymbol{\eta} \in (H^1(\Omega))^3 \mid \boldsymbol{\eta} = \mathbf{0} \quad \text{on } \partial\Omega_u \right\} \quad (21)$$

and the result is integrated over the domain Ω . Finally, application of Green's theorem leads to the *weak form of equilibrium*

$$g(\sigma_t, \eta) = \int_{\Omega} \sigma_t : \text{grad } \eta \, dv - \int_{\Omega} \rho \bar{b} \cdot \eta \, dv - \int_{\partial\Omega_e} \bar{t}_t \cdot \eta \, da = 0 \quad t \in \mathcal{I}. \tag{22}$$

Note, that in view of a finite-element displacement method the stresses σ_t are defined to be dependent on the displacement field u_t , i.e.

$$\sigma_t := \hat{\sigma}(u_t) \quad t \in \mathcal{I}. \tag{23}$$

Let

$$\Omega = \bigcup_{e=1}^{NE} \Omega_e \tag{24}$$

define the discretization of Ω into NE finite elements, and let $u_{t,h}$ be the approximation of u_t , where $u_{t,h} = \mathbf{N}V_t \in \mathcal{V}_h \subset \mathcal{V}$, $\mathbf{N} \in \mathcal{V}_h$ are shape-functions, and V_t is a vector of nodal displacements. Thus from equation (22) the condition for equilibrium

$$R(V_t) = \underbrace{\bigcup_{e=1}^{NE} \int_{\Omega_e} \mathbf{B}^T \hat{\sigma}(V_t) \, d\Omega}_{R^i(V_t)} - \underbrace{\left\{ \bigcup_{e=1}^{NE} \int_{\Omega_e} \mathbf{N}^T \rho \bar{b} \, d\Omega + \int_{\partial\Omega_e} \mathbf{N}^T \bar{t}_t \, \partial\Omega \right\}}_P \stackrel{!}{=} 0 \quad t \in \mathcal{I} \tag{25}$$

is derived, where \mathbf{B} is the strain–displacement matrix in standard notation.

For determination of the displacements V_t and the stresses $\hat{\sigma}(V_t)$ an incremental strategy is necessary. Let N be the number of time steps $\Delta t_{k+1} = t_{k+1} - t_k$, $k = 0, \dots, N - 1$, $t_0 = 0$, $t_N = T$, and let

$$\Delta V_{k+1} = V_{k+1} - V_k \quad k = 0, \dots, N - 1 \tag{26}$$

be incremental displacements. Then equation (25) is replaced by

$$R_{k+1}(\Delta V_{k+1}) = \underbrace{\bigcup_{e=1}^{NE} \int_{\Omega_e} \mathbf{B}^T \hat{\sigma}(\Delta V_{k+1}) \, d\Omega}_{R^i_{k+1}(\Delta V_{k+1})} - \underbrace{\left\{ \bigcup_{e=1}^{NE} \int_{\Omega_e} \mathbf{N}^T \rho \bar{b} \, d\Omega + \int_{\partial\Omega_e} \mathbf{N}^T \bar{t}_{k+1} \, \partial\Omega \right\}}_{P_{k+1}} \stackrel{!}{=} 0 \tag{27}$$

$$k = 0, \dots, N - 1.$$

The unknown stresses $\hat{\sigma}(\Delta V_{k+1})$ are obtained by time integration of the evolution equations (7) and (8) with respect to the basic equations (3)–(5) at any Gaussian point x_{ig} , $ig = 1, \dots, Ng$. Let

$$\sigma_{k+1} := \hat{\sigma}(\Delta V_{k+1}) \tag{28}$$

then, by use of a mid-point rule the following equations are obtained:

$$\Delta \varepsilon_{ig,k+1} = \Delta \varepsilon_{ig,k+1}^{el} + \Delta \varepsilon_{ig,k+1}^{in} \tag{29}$$

$$q_{ig,k+1} = q_{ig,k} + \Delta q_{ig,k+1} \tag{30}$$

$$ig = 1, \dots, Ng \quad k = 0, \dots, N - 1$$

with

$$\Delta \varepsilon_{ig,k+1} = \mathbf{B}_{ig} \Delta \mathbf{V}_{k+1} \quad (31)$$

$$\Delta \varepsilon_{ig,k+1}^{\text{el}} = \mathbf{C}^{-1} (\sigma_{ig,k+1} - \sigma_{ig,k}) \quad (32)$$

$$\Delta \varepsilon_{ig,k+1}^{\text{in}} = \Delta t_{k+1} \dot{\varepsilon}_{ig,k+1/2}^{\text{in}} (\sigma_{ig,k+1}, \mathbf{q}_{ig,k+1}) \quad (33)$$

$$\Delta \mathbf{q}_{ig,k+1} = \Delta t_{k+1} \dot{\mathbf{q}}_{ig,k+1/2} (\sigma_{ig,k+1}, \mathbf{q}_{ig,k+1}). \quad (34)$$

By definition of a vector of process variables $\mathbf{Y}_{ig,k+1} := [\sigma_{ig,k+1}, \mathbf{q}_{ig,k+1}]$, by multiplication of equation (29) with the elasticity matrix, and by use of equation (30) we thus can formulate the following non-linear system of equations for any Gaussian point \mathbf{x}_{ig} :

$$\mathbf{G}(\mathbf{Y}_{ig,k+1}) := \begin{bmatrix} g_1 \\ g_2 \end{bmatrix} := \begin{bmatrix} \mathbf{C} \Delta \varepsilon_{ig,k+1}^{\text{ges}} - \sigma_{ig,k+1} + \sigma_{ig,k} - \mathbf{C} \Delta \varepsilon_{ig,k+1}^{\text{in}} \\ \mathbf{q}_{ig,k+1} - \mathbf{q}_{ig,k} - \Delta \mathbf{q}_{ig,k+1} \end{bmatrix} \stackrel{!}{=} \mathbf{0} \quad (35)$$

$ig = 1, \dots, NG \quad k = 0, \dots, N-1.$

For solution of the direct problem in discretized form, basically, equations (27) and (35) have to be solved. The definition (28) for the displacement \mathbf{V}_k as *independent variables* and the stresses σ_k as *dependent variables* implies the following solution strategy: the FE analysis contains an outer loop, the global iteration for determination of \mathbf{V}_{k+1} , and an inner loop, the local iteration at any Gaussian point for determination of the process variables $\sigma_{ig,k+1}$ and $\mathbf{q}_{ig,k+1}$.

3.2. Local iteration

To simplify notations the index ig will be neglected in this section. The aim of the local iteration is to determine the *process variables* $\mathbf{Y}_{k+1} := [\sigma_{k+1}, \mathbf{q}_{k+1}]$ for given $\Delta \varepsilon_{k+1} = \mathbf{B} \Delta \mathbf{V}_{k+1}$ such that equation (35) is satisfied. By use of a Newton method the iteration scheme is defined as

$$\mathbf{Y}_{k+1}^{j+1} = \mathbf{Y}_{k+1}^j - \alpha^j [\mathbf{J}^j]^{-1} \mathbf{G}^j(\mathbf{Y}_{k+1}) \quad (36)$$

where

$$\mathbf{J} = \frac{\partial \mathbf{G}(\mathbf{Y}_{k+1})}{\partial \mathbf{Y}_{k+1}} \quad (37)$$

is the Jacobian of $\mathbf{G}(\mathbf{Y}_{k+1})$. In the case of the material law of Steck, the result for \mathbf{J} is given in subsection A.1 of the appendix.

We make the following remarks.

1. The process vector \mathbf{Y}_{k+1} consists of values of different size. Therefore it is necessary to scale the system of equations. In our program scaling was carried out with the diagonals of the Jacobian $\mathbf{J}^{(j=0)}$.

2. In order to achieve global convergence, a line-search parameter α^j is determined at each iteration step. For this we require that the merit function $\|\mathbf{G}\|$ decreases at each iteration step j (Dennis and Schnabel in [3]). However, sometimes numerical tests showed very small values for α , thus slowing down the convergence. Therefore we applied a modification of Grippo *et al* [5], where every K steps cycles are introduced into the iteration scheme, in which no line search is done or a different merit function is used (for further details see [5]).

3. The special case of a plane-stress problem can easily be implemented in an existing code, if the process vector is defined as $\mathbf{Y}_{k+1} := [\sigma_{x,k+1}, \sigma_{y,k+1}, \tau_{k+1}, \Delta \varepsilon_{z,k+1}, \mathbf{q}_{k+1}]^T$.

3.3. Global iteration

The solution of equation (27) is obtained according to

$$\Delta V_{k+1}^{j+1} = \Delta V_{k+1}^j - \alpha^j [\mathbf{K}_T^j]^{-1} \mathbf{R}_{k+1}^j \quad (38)$$

where the Jacobian of the residual vector

$$\mathbf{K}_T = \frac{d\mathbf{R}_{k+1}}{d\Delta\mathbf{V}_{k+1}} = \bigcup_{e=1}^{NE} \int_{\Omega_e} \mathbf{B}^T \frac{d\sigma_{k+1}}{d\Delta\epsilon_{k+1}} \mathbf{B} d\Omega \quad (39)$$

is known as the consistent tangent matrix. Therefore the term $\mathbf{C}_T = d\sigma_{k+1}/d\Delta\epsilon_{k+1}$ has to be determined. In view of the fact that both the stresses σ_{k+1} and the internal variables depend on $\Delta\epsilon_{k+1}$, a condensation of q_{k+1} is done as follows. We begin with the definition of an implicit function (compare the local iteration)

$$g_1(\Delta\epsilon_{k+1}) = \mathbf{C}\Delta\epsilon_{k+1} - \sigma_{k+1} + \sigma_k - \mathbf{C}\Delta\epsilon_{k+1}^{\text{in}} = \mathbf{0} \quad (40)$$

$$= g_1(\Delta\epsilon_{k+1}, \sigma_{k+1}(\Delta\epsilon_{k+1}), q_{k+1}(\Delta\epsilon_{k+1})) \quad (41)$$

$$=: \bar{g}_1(\Delta\epsilon_{k+1}, \sigma_{k+1}(\Delta\epsilon_{k+1}), q_{k+1}(\sigma_{k+1}(\Delta\epsilon_{k+1}))) \quad (42)$$

$$=: \bar{\bar{g}}_1(\Delta\epsilon_{k+1}, \sigma_{k+1}(\Delta\epsilon_{k+1})). \quad (43)$$

The total differential of $\bar{\bar{g}}_1$ is given by

$$\frac{d\bar{\bar{g}}_1}{d\Delta\epsilon_{k+1}} = \frac{\partial\bar{\bar{g}}_1}{\partial\Delta\epsilon_{k+1}} + \frac{\partial\bar{\bar{g}}_1}{\partial\sigma_{k+1}} \frac{d\sigma_{k+1}}{d\Delta\epsilon_{k+1}} = 0. \quad (44)$$

Thus the unknown term is found to be

$$\frac{d\sigma_{k+1}}{d\Delta\epsilon_{k+1}} = - \left[\frac{\partial\bar{\bar{g}}_1}{\partial\sigma_{k+1}} \right]^{-1} \frac{\partial\bar{\bar{g}}_1}{\partial\Delta\epsilon_{k+1}} \quad (45)$$

where

$$\frac{\partial\bar{\bar{g}}_1}{\partial\Delta\epsilon_{k+1}} = \mathbf{C} \quad \frac{\partial\bar{\bar{g}}_1}{\partial\sigma_{k+1}} = \frac{\partial\bar{g}_1}{\partial\sigma_{k+1}} + \frac{\partial\bar{g}_1}{\partial q_{k+1}} \frac{dq_{k+1}}{d\sigma_{k+1}}. \quad (46)$$

For determination of $dq_{k+1}/d\sigma_{k+1}$ we define

$$g_2 = q_{k+1} - q_k - \Delta q_{k+1} \quad (47)$$

$$=: \bar{g}_2(\sigma_{k+1}, q_{k+1}(\sigma_{k+1})) \quad (48)$$

and we deduce

$$\frac{dq_{k+1}}{d\sigma_{k+1}} = - \left[\frac{\partial\bar{g}_2}{\partial q_{k+1}} \right]^{-1} \frac{\partial\bar{g}_2}{\partial\sigma_{k+1}}. \quad (49)$$

To summarize, for the determination of \mathbf{K}_T

1. The partial differentials of g_1 and g_2 with respect to the process variables σ_{k+1} , q_{k+1} (i.e. the Jacobian in the local iteration) have to be provided,
2. The internal variables q_{k+1} are condensed, and
3. The special case of plane-stress problems can be treated by further condensation.

The result for \mathbf{C}_T in the case of the material law due to Steck is presented in subsection A.2 of the appendix.

4. On solution of the inverse problem

4.1. Discrete formulation and solution strategy

We assume that experimental data at points $x_p \in \Omega$, $p = 1, \dots, MP$ for discrete time values t_k , $k = 1, \dots, N$ are given. Thus a possible function for the inverse problem can be as follows:

$$f = \sum_{p=1}^{MP} \sum_{k=1}^N \|V_{k,p} - \bar{V}_{k,p}\|^2 \longrightarrow \min. \quad (50)$$

Additionally, equilibrium conditions have to be satisfied. From equation (27) of the direct problem we deduce the following constraints:

$$R_k(\kappa, \Delta V_k) = \mathbf{0} \quad k = 1, \dots, N. \quad (51)$$

Further constraints for the material parameter κ (e.g. conditions between the material parameters, upper and lower side constraints) shall be denoted by

$$h_1(\kappa) = \mathbf{0} \quad (52)$$

$$h_2(\kappa) \leq \mathbf{0}. \quad (53)$$

Thus equations (50)–(53) define the non-linear optimization problem for the inverse problem in discretized form, where $(\kappa, \Delta V_k, k = 1, \dots, N)$ is the set of unknowns. In general this problem is characterized by its large dimension. Note that the above type of problem is very similar to problems in structural optimization (see e.g. [1, 11]). For this kind of problem the following solution strategy is suitable.

For two reasons it is advisable to separate a finite-element calculation for solution of the direct problem from the optimization process.

- The existing finite-element code for solution of the direct problem should not be changed too much.
- In general $\dim(\kappa) \ll \dim(\Delta V_k, k = 1, \dots, N)$.

The separation is possible via the following definition.

- The material parameters are *independent variables*.
- The displacements are *dependent variables*, i.e. $\Delta V_k = \Delta \hat{V}_k(\kappa)$, $k = 1, \dots, N$.

The resulting optimization problem is given by

$$\begin{aligned} f(\kappa, x(\kappa)) &\longrightarrow \min_{\kappa} \\ h_1(\kappa, x(\kappa)) &= \mathbf{0} \\ h_2(\kappa, x(\kappa)) &\leq \mathbf{0} \end{aligned} \quad (54)$$

where $x(\kappa) := \{\Delta V_k, k = 1, \dots, N\}$ is defined to be the solution of the direct problems

$$R_{k+1}(\kappa, \Delta V_{k+1}(\kappa)) = \mathbf{0} \quad k = 0, \dots, N - 1 \quad (55)$$

for given (frozen) κ in a finite-element analysis.

It can be seen that the above strategy reduces the dimension of the optimization problem significantly to $\dim(\kappa)$. However, it should be noted that the functions of interest depend on κ both explicitly and implicitly.

As a practical consequence it follows that *in an optimization process on solution of the problem (54) a complete non-linear finite-element analysis has to be carried out for any set of material parameters κ .*

Optimization algorithms for problem (54) can be classified into methods which use only function values (e.g. the evolution strategy) and methods which use function values and gradients (e.g. the SQP method according to Schittkowski [13] or a projection algorithm due to Bertsekas [2]). Since in general the first kind of method is not efficient due to the large number of function evaluations the second kind will be used. Therefore the gradient of the objective function has to be determined in a *sensitivity analysis*.

4.2. Sensitivity analysis

For explanation of the sensitivity analysis the following objective function shall be considered:

$$f(\kappa) = \sum_{i=1}^N \sum_{p=1}^{MP} \|V_{i,p}(\kappa) - \bar{V}_{i,p}\|^2. \quad (56)$$

Thus the gradient is given by

$$\frac{df}{d\kappa} = 2 \sum_{i=1}^N \sum_{p=1}^{MP} (V_{i,p}(\kappa) - \bar{V}_{i,p}) \frac{dV_{i,p}}{d\kappa} \quad (57)$$

$$= 2 \sum_{i=1}^N \sum_{p=1}^{MP} (V_{i,p}(\kappa) - \bar{V}_{i,p}) \sum_{k=0}^{i-1} \frac{d\Delta V_{k+1,i,p}}{d\kappa} \quad (58)$$

where in equation (58) we use the fact that the displacements are the result of an incremental step-by-step calculation. Next, for simplicity of notation we shall neglect the indices i, p . We start with the implicit function (55). The total differential is given by

$$\frac{dR_{k+1}}{d\kappa} = \frac{\partial R_{k+1}}{\partial \kappa} + \underbrace{\frac{\partial R_{k+1}}{\partial \Delta V_{k+1}}}_{\mathbf{K}_T} \frac{d\Delta V_{k+1}}{d\kappa} = \mathbf{0} \quad (59)$$

and solving this equation for the unknowns yields

$$\frac{d\Delta V_{k+1}}{d\kappa} = -[\mathbf{K}_T]^{-1} \frac{\partial R_{k+1}}{\partial \kappa}. \quad (60)$$

For evaluation of equation (60) it has to be taken into account, that a factorization of \mathbf{K}_T is available from solution of the direct problem [1, 11]. Now it remains to determine the *partial load vector*

$$\frac{\partial R_{k+1}}{\partial \kappa} = \bigcup_{e=1}^{NE} \int_{\Omega_e} \mathbf{B}^T \frac{d\sigma_{k+1}}{d\kappa} d\Omega. \quad (61)$$

For this task a similar procedure as for determination of \mathbf{K}_T in equation (39) can be applied, i.e. the internal variables are condensed. Again, the basis is an implicit function

$$\begin{aligned} g_1(\kappa) &= \mathbf{C}\Delta\epsilon_{k+1} - \sigma_{k+1} + \sigma_k - \mathbf{C}\Delta\epsilon_{k+1}^{\text{in}} = \mathbf{0} \\ &= g_1(\kappa, \mathbf{q}_{k+1}(\kappa), \sigma_{k+1}(\kappa), \mathbf{Y}_k(\kappa)) \\ &=: \bar{g}_1(\kappa, \mathbf{q}_{k+1}(\kappa), \sigma_{k+1}(\kappa), \mathbf{q}_{k+1}(\sigma_{k+1}(\kappa)), \mathbf{Y}_k(\kappa), \mathbf{q}_{k+1}(\mathbf{Y}_k(\kappa))) \\ &=: \bar{\bar{g}}_1(\kappa, \sigma_{k+1}(\kappa), \mathbf{Y}_k(\kappa)) \end{aligned} \quad (62)$$

where the total differential is given by

$$\frac{d\bar{\bar{g}}_1}{d\kappa} = \frac{\partial \bar{\bar{g}}_1}{\partial \kappa} + \frac{\partial \bar{\bar{g}}_1}{\partial \mathbf{Y}_k} \frac{d\mathbf{Y}_k}{d\kappa} + \frac{\partial \bar{\bar{g}}_1}{\partial \sigma_{k+1}} \frac{d\sigma_{k+1}}{d\kappa} = \mathbf{0}. \quad (63)$$

Solving for the unknowns yields

$$\frac{d\sigma_{k+1}}{d\kappa} = - \left[\underbrace{\frac{\partial \bar{g}_1}{\partial \sigma_{k+1}}}_1 \right]^{-1} \left(\underbrace{\frac{\partial \bar{g}_1}{\partial \kappa}}_2 + \underbrace{\frac{\partial \bar{g}_1}{\partial Y_k}}_3 \underbrace{\frac{dY_k}{d\kappa}}_4 \right) \quad (64)$$

with

$$\begin{aligned} \text{Term 1 : } & \frac{\partial \bar{g}_1}{\partial \sigma_{k+1}} = \frac{\partial \bar{g}_1}{\partial \sigma_{k+1}} + \frac{\partial \bar{g}_1}{\partial q_{k+1}} \underbrace{\frac{dq_{k+1}}{d\sigma_{k+1}}}_5 \\ \text{Term 2 : } & \frac{\partial \bar{g}_1}{\partial \kappa} = \frac{\partial \bar{g}_1}{\partial \kappa} + \frac{\partial \bar{g}_1}{\partial q_{k+1}} \underbrace{\frac{dq_{k+1}}{d\kappa}}_6 \\ \text{Term 3 : } & \frac{\partial \bar{g}_1}{\partial Y_k} = \frac{\partial \bar{g}_1}{\partial Y_k} + \frac{\partial \bar{g}_1}{\partial q_{k+1}} \underbrace{\frac{dq_{k+1}}{dY_k}}_7. \end{aligned} \quad (65)$$

Terms 5–7 are derived from the condition $g_2 = 0$ as

$$\begin{aligned} \text{Term 5 : } & \frac{dq_{k+1}}{d\sigma_{k+1}} = - \left[\frac{\partial \bar{g}_2}{\partial q_{k+1}} \right]^{-1} \frac{\partial \bar{g}_2}{\partial \sigma_{k+1}} \\ \text{Term 6 : } & \frac{dq_{k+1}}{d\kappa} = - \left[\frac{\partial \bar{g}_2}{\partial q_{k+1}} \right]^{-1} \frac{\partial \bar{g}_2}{\partial \kappa} \\ \text{Term 7 : } & \frac{dq_{k+1}}{dY_k} = - \left[\frac{\partial \bar{g}_2}{\partial q_{k+1}} \right]^{-1} \frac{\partial \bar{g}_2}{\partial Y_k}. \end{aligned} \quad (66)$$

For determination of term 4 an implicit function is defined at the previous time step as

$$\mathbf{G}_k := \begin{bmatrix} g_{1,k} \\ g_{2,k} \end{bmatrix} := \begin{bmatrix} \mathbf{C}\Delta\varepsilon_k - \sigma_k + \sigma_{k-1} - \mathbf{C}\Delta\varepsilon_k^{\text{in}} \\ q_k - q_{k-1} - \Delta t_k \dot{q}_{k-1/2} \end{bmatrix} \quad (67)$$

$$= \mathbf{G}_k(\kappa, Y_k(\kappa), Y_{k-1}(\kappa), \Delta\varepsilon_k(\kappa)) = 0. \quad (68)$$

For this function the total differential is given by

$$\frac{d\mathbf{G}_k}{d\kappa} = \frac{\partial \mathbf{G}_k}{\partial \kappa} + \frac{\partial \mathbf{G}_k}{\partial Y_k} \frac{dY_k}{d\kappa} + \frac{\partial \mathbf{G}_k}{\partial Y_{k-1}} \frac{dY_{k-1}}{d\kappa} + \frac{\partial \mathbf{G}_k}{\partial \Delta\varepsilon_k} \frac{d\Delta\varepsilon_k}{d\kappa} \quad (69)$$

and we deduce

$$\frac{dY_k}{d\kappa} = - \left[\underbrace{\frac{\partial \mathbf{G}_k}{\partial Y_k}}_8 \right]^{-1} \left(\underbrace{\frac{\partial \mathbf{G}_k}{\partial \kappa}}_9 + \underbrace{\frac{\partial \mathbf{G}_k}{\partial Y_{k-1}} \frac{dY_{k-1}}{d\kappa}}_{10} + \underbrace{\frac{\partial \mathbf{G}_k}{\partial \Delta\varepsilon_k} \frac{d\Delta\varepsilon_k}{d\kappa}}_{12} + \underbrace{\frac{\partial \mathbf{G}_k}{\partial \Delta\varepsilon_k} \frac{d\Delta\varepsilon_k}{d\kappa}}_{13} \right). \quad (70)$$

Concerning terms 8–13 the following remarks are made.

Term 8: This term corresponds to the Jacobian \mathbf{J} of the local iteration, and thus it is available.

Term 9: For this term the partial derivatives of the function \mathbf{G} with respect to the material parameters κ are required. For the special case of Steck's model the result is given in subsection A.3 of the appendix.

Term 10: Note the simple relation

$$\frac{\partial \mathbf{G}_k}{\partial \mathbf{Y}_{k-1}} = \frac{\partial \mathbf{G}_k}{\partial \mathbf{Y}_k} - 2\mathbf{I}. \quad (71)$$

Term 11: This term can be adopted from the previous time step. Thus it can be seen that the sensitivity analysis yields a *recursion formula*. It is not necessary to take into account results from time steps which are before the previous step.

Term 12: This term corresponds to the elasticity matrix \mathbf{C} .

Term 13:

$$\frac{d\Delta \varepsilon_k}{d\kappa} = \mathbf{B} \frac{d\Delta \mathbf{V}_k}{d\kappa}.$$

The sensitivity analysis may be summarized as follows.

1. Firstly the partial differentials of the functions g_1 and g_2 with respect to κ , \mathbf{Y}_{k+1} , \mathbf{Y}_k and $\Delta \varepsilon_{k+1}$ have to be provided.
2. The internal variables q_{k+1} are condensed.
3. As a result a *recursion formula* is obtained.
4. In the case of homogeneous 1D problems (i.e. in the absence of field equations) the remarks in points 1–3 are also valid.

The following remarks are made on numerical implementation.

1. The numerical implementation—including condensation—can be carried out *independently of the specific material law* if the partial derivatives of the functions g_1 and g_2 are provided. This fact is of importance for implementation of further material laws.
2. The gradient is calculated in parallel to the finite-elemente analysis by doing an update of both the process variables \mathbf{Y}_k and its derivatives $d\mathbf{Y}_k/d\kappa$ at each time step. Thus storing results for $d\mathbf{Y}_k/d\kappa$ at all time steps is avoided.

5. Examples

5.1. Stationary creep for aluminium according to Servi and Grant

In the first example the iteration behaviours of an evolution strategy and a gradient method, the Bertsekas algorithm, are compared. The material law and the experimental data for aluminium according to Servi and Grant [15] are taken from [8]. In this thesis parameters were identified for tension tests with homogeneous stresses and deformations. The material law is given for the rates of strains in logarithmic form as

$$\ln(\dot{\varepsilon}_s) = \kappa_1 - \frac{\kappa_2 U_0}{RT} + \kappa_3 \ln \left[\operatorname{sh} \left(\frac{\kappa_4 \sigma}{RT} \right) \right] \quad (72)$$

where $R = 8.314 \text{ J mol}^{-1} \text{ K}^{-1}$ and $U_0 = 149 \text{ kJ mol}^{-1}$.

The following least-squares function has to be minimized:

$$f(\kappa) = \sum_{i=1}^m \left[\ln(\dot{\varepsilon}_{s,i}) - \ln(\hat{\varepsilon}_{s,i}) \right]^2. \quad (73)$$

The gradient is simply given by

$$\frac{df(\kappa)}{d\kappa} = 2 \sum_{i=1}^m \left[\ln(\dot{\varepsilon}_{s,i}) - \ln(\hat{\varepsilon}_{s,i}) \right] \frac{d(\ln(\dot{\varepsilon}_{s,i}))}{d\kappa} \quad (74)$$

with

$$\frac{d(\ln(\dot{\epsilon}_{s,i}))}{d\kappa_1} = 1 \quad (75)$$

$$\frac{d(\ln(\dot{\epsilon}_{s,i}))}{d\kappa_2} = \frac{U_0}{RT} \quad (76)$$

$$\frac{d(\ln(\dot{\epsilon}_{s,i}))}{d\kappa_3} = \ln \left[\text{sh} \left(\frac{\kappa_4 \sigma}{RT} \right) \right] \quad (77)$$

$$\frac{d(\ln(\dot{\epsilon}_{s,i}))}{d\kappa_4} = \kappa_3 \text{ch} \left(\frac{\kappa_4 \sigma}{RT} \right) \frac{\sigma/RT}{\text{sh}(\kappa_4 \sigma / RT)} \quad (78)$$

Table 1. Aluminium according to Servi and Grant: starting vector, solution vector and corresponding function values for three optimization algorithms.

	Starting vector κ^1	Solution vector κ^*
κ	10.0	25.170
	1.0	1.085
	10.0	3.815
	1.0	0.371
$f(\kappa)$	57391.27	4.042

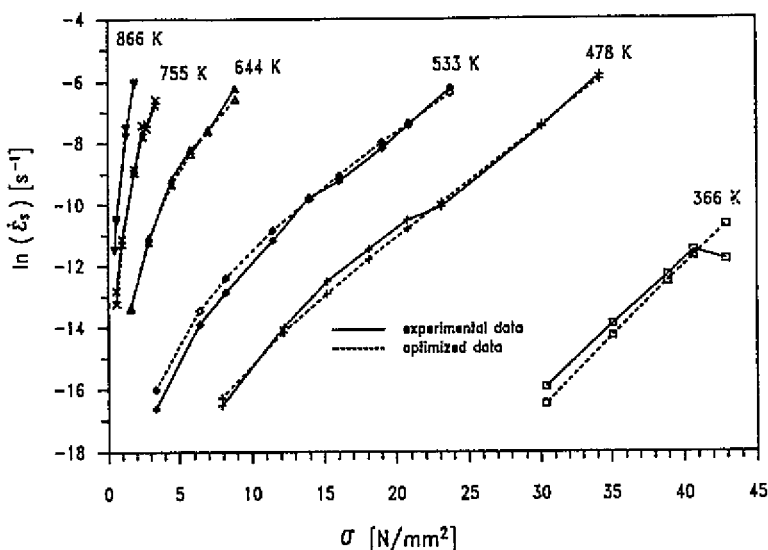


Figure 1. Aluminium according to Servi and Grant: experimental data and optimized data for six different temperatures.

For optimization, three methods, a one-level evolution strategy, a multi-level evolution strategy and a Bertsekas algorithm, were compared. Both the starting vector and the solution vector were identical for all computer runs (compare table 1). In figure 1, both the experimental data and the optimized data for the strains with six different temperatures are shown. In table 2 the CPU time, the number of function evaluations and the number

Table 2. Aluminium according to Servi and Grant: comparison of three optimization algorithms for CPU time, number of function evaluations and number of iterations.

	CPU time (s)	Number of function evaluations	Number of iterations
One-level evolution strategy	154	55 386	13 859
Multi-level evolution strategy	47	36 421	1 217
Bertsekas algorithm	<1	29	25

of iterations are compared for all computer runs. For this example the advantage of the Bertsekas algorithm is obvious.

5.2. Numerical tests for Steck's model for a 1D tension specimen

In this section the material law due to Steck in its one-dimensional form is used for numerical tests. Therefore, using the data for aluminium, Al 99.999, of table 3 and table 4, creep curves were calculated which are shown in figure 2. For time integration the second-order mid-point rule was applied. The results obtained are regarded as experimental data for the following tests.

Table 3. 1D specimen: material parameters for the model of Steck (Al 99.999).

Activation energy	U_0	149	kJ mol^{-1}
Gas constant	R	8.315×10^3	$\text{kJ mol}^{-1} \text{K}^{-1}$
Melting temperature	T_m	933(660)	K ($^{\circ}\text{C}$)
	$0.5T_m$	466(193)	K ($^{\circ}\text{C}$)
Material parameters	c_1	2.43×10^{11}	$\text{kJ mol}^{-1} \text{s}^{-1}$
	c_2	1.41×10^4	$\text{kJ mol}^{-1} \text{s}^{-1}$
	λ'	1.05×10^{-2}	mol kJ^{-1}
	α	0.951	
	β	9.19	
	κ	0.275	
	ΔV	1.15	$\text{kJ mm}^2 \text{N}^{-1} \text{mol}^{-1}$

Table 4. 1D specimen: data for creep curve determination with Steck's model. Number of time steps, 50; size of each time step, $\Delta t = 80$ s; number of stresses, 10.

	1	2	3	4	5	6	7	8	9	10
σ (MPa)	4.7	4.5	3.5	3.2	2.5	2.0	1.8	1.5	1.2	1.0
T (K)	660	670	680	690	700	710	720	730	740	750

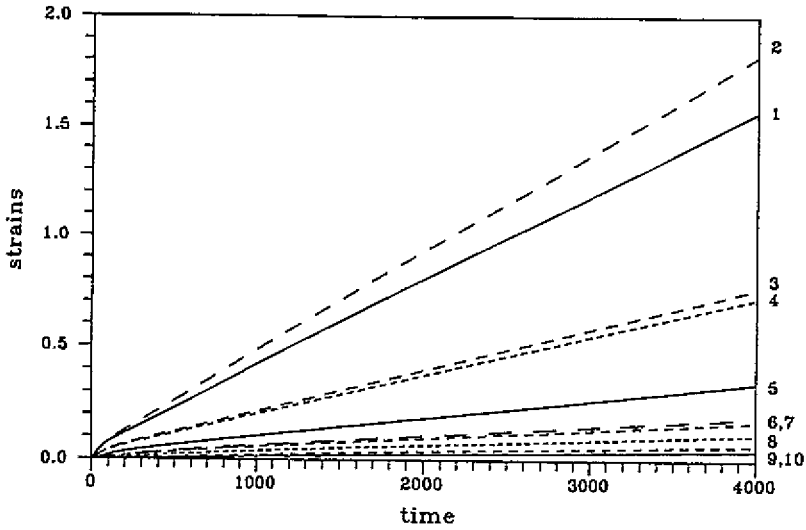


Figure 2. 1D specimen: 10 creep curves using Steck's model with data according to tables 3 and 4.

As an objective function for an inverse problem the following least-squares function was considered:

$$f(\kappa) = \sum_{k=1}^{10} \sum_{j=1}^{50} \frac{(\varepsilon_{k,j}(\kappa) - \bar{\varepsilon}_{k,j})^2}{\bar{\varepsilon}_{k,j}^2} \rightarrow \min. \quad (79)$$

For minimization of the objective function the Bertsekas algorithm was used. Two computer runs were started using different starting vectors as shown in table 5. The solution vectors of both runs are given in table 6. It can be seen, that both runs give the same solution, which are identical to the vector of table 3. In table 7 some results are presented concerning the number of iterations, the number of function evaluations and the CPU time. The iteration behaviour of the objective function is shown in figure 3. Note that the evolution strategy did not give satisfactory results after 3 h.

Table 5. 1D specimen: starting vectors of two computer runs for identification of parameters.

Computer run	1	2	
c_1	1	1 674 535	$\text{kJ mol}^{-1} \text{s}^{-1}$
c_2	1.0	14 390.5	$\text{kJ mol}^{-1} \text{s}^{-1}$
λ'	1.0	1.0516×10^{-2}	mol kJ^{-1}
α	1.0	1.196	
β	1.0	12.6	
κ	1.0	0.147	
ΔV	1.0	2.28×10^{-2}	$\text{kJ mm}^2 \text{N}^{-1} \text{mol}^{-1}$

5.3. Compact tension specimen

In this section our optimization algorithm is tested for parameter identification in the context of a finite-element method. The specific example is a compact tension (CT) specimen as

Table 6. 1D specimen: target and obtained values for the material parameters.

	Target	Obtained	
c_1	2.43×10^{11}	2.43×10^{11}	$\text{kJ mol}^{-1} \text{s}^{-1}$
c_2	1.41×10^4	1.41×10^4	$\text{kJ mol}^{-1} \text{s}^{-1}$
λ'	1.05×10^{-2}	1.05×10^{-2}	mol kJ^{-1}
α	0.951	0.951	
β	9.19	9.19	
κ	0.275	0.275	
ΔV	1.15	1.15	$\text{kJ mm}^2 \text{N}^{-1} \text{mol}^{-1}$

Table 7. 1D specimen: some results for two computer runs with the Bertsekas algorithm.

Computer run	1	2
Number of iterations	2783	3077
Number of function evaluations	4511	5390
cpu time (DN 10000) (min)	14.5	17.4

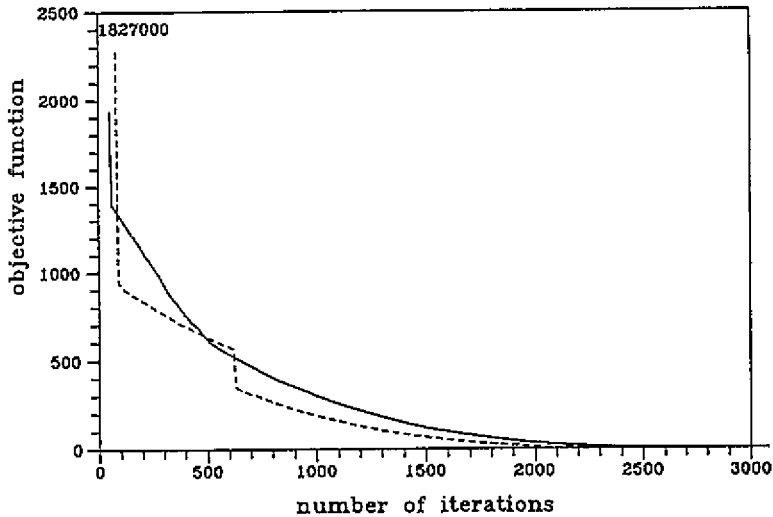


Figure 3. 1D specimen: iteration behaviour of the objective functions for the Bertsekas algorithm.

shown in figure 4. Of course, the deformations are below the limit of localization at the nodge. As a material law Steck's model is used. The discretization is shown in figure 5. It is the result of an adaptive refinement based on the Zienkiewicz-Zhu error estimator.

Conceptually we proceed in the same manner as in the previous example. Firstly a direct problem was solved with material data of table 3. Using 30 unequally spaced time steps we obtained creep curves for V_x and V_y at those points which are marked in figure 5. The results for the creep curves are shown in figure 6.

As an objective function the following least-squares function was examined:

$$f = \sum_{k=1}^{N=30} \sum_{j=1}^{MP=16} \left\| \frac{V_{k,j} - \bar{V}_{k,j}}{V_{k,j}^{\text{iter}=1} - \bar{V}_{k,j}} \right\|^2 \rightarrow \min. \quad (80)$$

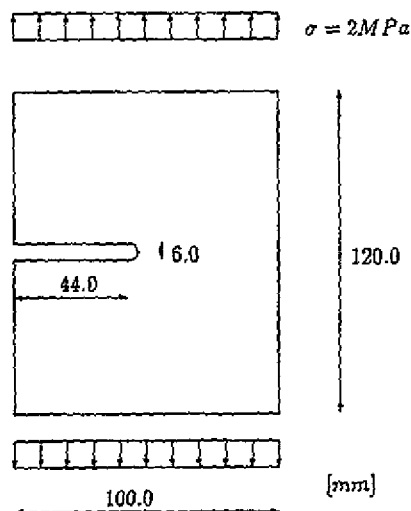


Figure 4. Geometry of a CT specimen.

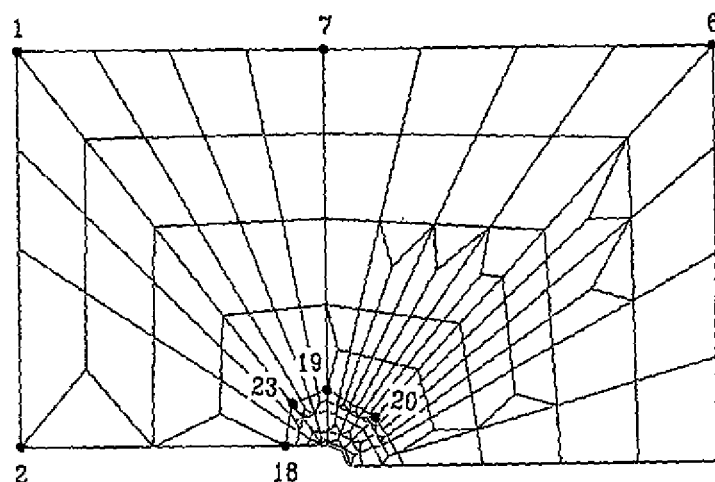


Figure 5. CT specimen: discretization after adaptive refinement, marking of eight data points.

Table 8. CT specimen: starting, target and obtained values for the material parameters.

	Starting	Target	Obtained	
c_1	10^8	2.43×10^{11}	2.37×10^8	$\text{kJ mol}^{-1} \text{s}^{-1}$
c_2	10^4	1.41×10^4	9.488×10^4	$\text{kJ mol}^{-1} \text{s}^{-1}$
λ'	1.0	1.05×10^{-2}	1.05×10^{-2}	mol kJ^{-1}
α	1.0	0.951	1.021	
β	10^4	9.19	9.19	
κ	1.0	0.275	0.275	
ΔV	1.0	1.15	1.15	$\text{kJ mm}^2 \text{N}^{-1} \text{mol}^{-1}$

For optimization an SQP method as described in [13] was applied. The iteration behaviour

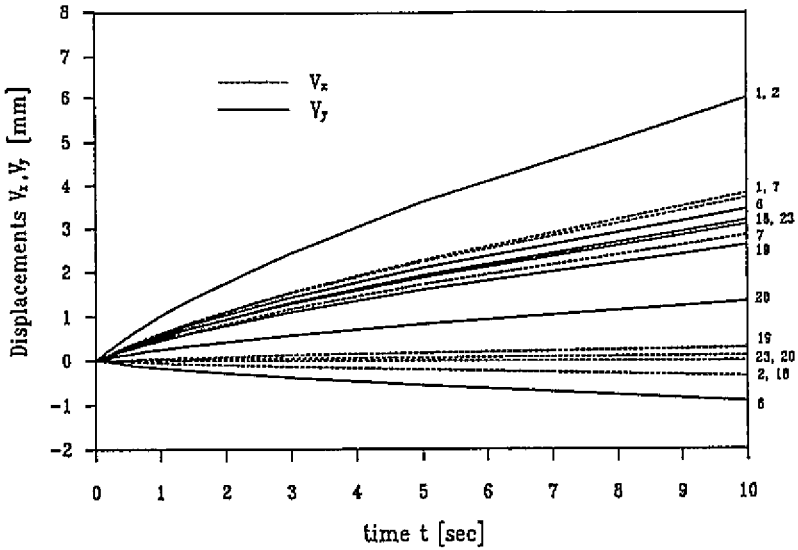


Figure 6. CT specimen: calculated creep curves with Steck's model; the numbers on the right-hand side correspond to the nodes in figure 5.

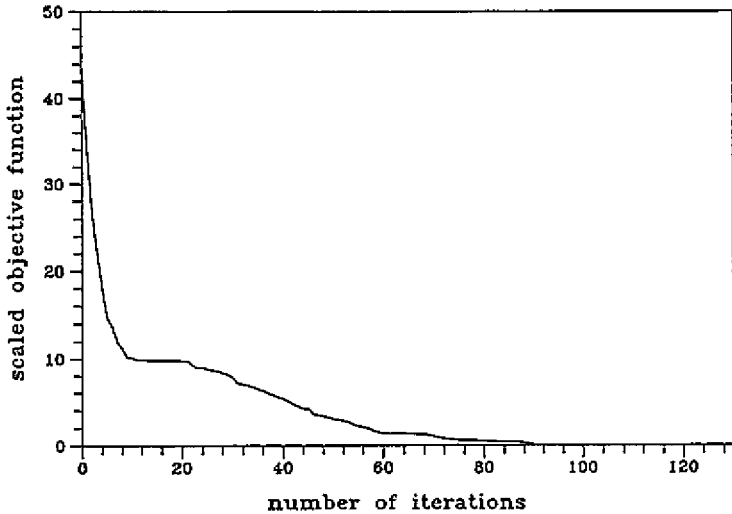


Figure 7. CT specimen: iteration behaviour of the scaled objective function for the SQP algorithm.

of the objective function is shown in figure 7. The number of iterations and the number of function evaluations are as follows:

number of iterations: 238
 number of function evaluations: 335.

In table 8 the starting values, the target values and the obtained values are shown. It can be seen that four material parameters of the obtained values are identical to the target values, whilst three values are different. This result and further tests indicate a dependence of the material parameters which did not occur in the previous example.

5.4. Discussion of the results

The results of the identification for the homogeneous test and for the CT specimen seem to be contradictory. Whilst in section 5.2 all parameters were recovered by the optimization process, we have a dependence of three parameters c_1 , c_2 and α in section 5.3. The reason is found in choosing the target functions: whereas in section 5.2 the experimental displacement–time curves were calculated for 10 different temperatures, only one temperature was used in the second case.

In order to clarify this, we examine equations (10) and (11), and, especially for constant temperatures, the expressions

$$c_1 \exp \left[- \left(1 - \frac{\alpha - 1}{\kappa} \frac{U_0}{RT} \right) \right] = \text{const}_1 \quad (81)$$

and

$$c_2 \exp \left[- \frac{\alpha U_0 - \beta F}{RT} \right] = \underbrace{c_2 \exp \left[- \frac{\alpha U_0}{RT} \right]}_{\text{const}_2} \exp \left[\frac{\beta F}{RT} \right]. \quad (82)$$

One recognizes that the terms const_i , $i = 1, 2$ contain three instead of two independent variables. Thus, it can be concluded that the material equation in the present form cannot be used in general for identification of material parameters. At the moment the equations are being modified for general requirements in collaboration with Professor Heck of the Technical University of Braunschweig.

6. Conclusions

It is obvious that the identification of material parameters of complex constitutive equations from various tests is an important requirement in order to obtain reliable simulations of inelastic responses of system components. Mathematically this task is usually a Hadamard problem.

Furthermore it could be shown that gradient methods are much more efficient than stochastic evolution strategies even in the case of homogeneous stress fields.

Finally it is an important issue that general identification methods for material parameters yield a verification of the constitutive equations for the domain of intended applications, or even a falsification. The consideration of field equations makes it suitable for model adaptivity describing different constitutive equations in different process areas.

The implementation of geometrical non-linearity including damage is in progress.

Appendix. The material law of Steck

A.1. Jacobian matrix \mathbf{J}

$$\frac{\partial g_1}{\partial \sigma_{k+1}} = \mathbf{C}^{-1} + \left(\frac{3}{2} e_1 - \frac{9 \Delta \varepsilon_{v,k+1}^{\text{in}}}{8 \sigma_{v,k+1/2}} \right) \mathbf{n}_{k+1/2} \mathbf{n}_{k+1/2}^T + \frac{3 \Delta \varepsilon_{v,k+1}^{\text{in}}}{4 \sigma_{v,k+1/2}} \left(\mathbf{1}^{4 \times 4} - \frac{1}{3} \mathbf{1}^4 \mathbf{1}^{4T} \right) \quad (83)$$

$$\frac{\partial g_1}{\partial F_{k+1}} = - \frac{3}{4RT} \Delta \varepsilon_{v,k+1}^{\text{in}} \mathbf{n}_{k+1/2} \quad (84)$$

$$\frac{\partial g_2}{\partial \sigma_{k+1}} = - \frac{1}{\lambda'} e_1 \mathbf{n}_{k+1/2} \quad (85)$$

$$\frac{\partial g_2}{\partial F_{k+1}} = 1 + \left(\frac{\Delta t_{k+1} c_2 \exp[-(\alpha U_0 - \beta F_{k+1/2})/RT] \beta}{2RT} - \frac{\Delta \varepsilon_{v,k+1}^{\text{in}}}{2\lambda' RT} \right) \quad (86)$$

with

$$\mathbf{1}^4 = [1, 1, 1, 0]^T \quad \mathbf{s}_{v,k+1/2} = \left(\mathbf{1}^{4 \times 4} - \frac{1}{3} \mathbf{1}^4 \mathbf{1}^{4T} \right) \boldsymbol{\sigma}_{k+1/2} \quad (87)$$

$$\mathbf{n}_{k+1/2} = \frac{1}{\sigma_{v,k+1/2}} \mathbf{s}_{v,k+1/2} \quad \sigma_{v,k+1/2} = \left(\frac{3}{2} \mathbf{s}_{v,k+1/2}^T \mathbf{s}_{v,k+1/2} \right)^{1/2}$$

$$\Delta \varepsilon_{v,k+1}^{\text{in}} = \Delta t_{k+1} \lambda' c_1 \exp[-(1 - [(\alpha - 1)/\kappa] U_0/RT)] \times \left(2 \sinh \left(\frac{\Delta V}{RT} \sigma_{v,k+1/2} \right) \right)^{1+1/\kappa} \exp \left(-\frac{F_{k+1/2}}{RT} \right) \quad (88)$$

$$e_1 = \frac{3 \Delta t_{k+1} \lambda' c_1 \exp[-(1 - [(\alpha - 1)/\kappa] U_0/RT)]^{1+1/\kappa}}{4 \left(2 \sinh \left(\frac{\Delta V}{RT} \sigma_{v,k+1/2} \right) \right)} \exp \left(-\frac{F_{k+1/2}}{RT} \right) \times \left(2 \sinh \left(\frac{\Delta V}{RT} \sigma_{v,k+1/2} \right) \right)^{1+1/\kappa} \left(2 \cosh \left(\frac{\Delta V}{RT} \sigma_{v,k+1/2} \right) \right) \frac{\Delta V}{RT} \quad (89)$$

$$e_2 = 1 - \frac{\Delta \varepsilon_{v,k+1}^{\text{in}}}{2RT + hc_2 \lambda' \exp[-(\alpha U_0 - \beta F_{k+1/2})/RT] + \Delta \varepsilon_{v,k+1}^{\text{in}}} \quad (90)$$

A.2. Consistent tangent matrix

$$\mathbf{C}_T = b_1 \mathbf{1}^{3 \times 3} + b_2 \mathbf{1}^3 \mathbf{1}^{3T} + b_3 \mathbf{n}_{k+1/2} \mathbf{n}_{k+1/2}^T \quad (91)$$

with

$$b_1 = \frac{1}{a_1} \quad (92)$$

$$b_2 = -\frac{b_1 a_2}{a_1 + 3a_2} \quad (93)$$

$$b_3 = -\frac{3b_1 a_3}{3a_1 + 2a_3} \quad (94)$$

and

$$a_1 = \frac{1}{2\mu} + \frac{3\Delta \varepsilon_{v,k+1}^{\text{in}}}{4\sigma_{v,k+1/2}} \quad (95)$$

$$a_2 = -\frac{\nu}{E} - \frac{1\Delta \varepsilon_{v,k+1}^{\text{in}}}{4\sigma_{v,k+1/2}} \quad (96)$$

$$a_3 = 3e_1 e_2 - \frac{9\Delta \varepsilon_{v,k+1}^{\text{in}}}{8\sigma_{v,k+1/2}} \quad (97)$$

A.3. Derivatives with respect to the material parameters

We define $\boldsymbol{\kappa} := [\lambda', \Delta V, \alpha, \kappa, c_1, \beta, c_2]^T$

$$\frac{\partial g_1}{\partial \kappa_i} = -3\mu \mathbf{n}_{k+1/2} \frac{\partial \Delta \varepsilon_{v,k+1}^{\text{in}}}{\partial \kappa_i} \quad i = 1, \dots, 7. \quad (98)$$

$$\frac{\partial g_2}{\partial \kappa_1} = 0 \quad (99)$$

$$\frac{\partial g_2}{\partial \kappa_i} = -\frac{1}{\lambda'} \frac{\partial \Delta \varepsilon_{v,k+1}^{\text{in}}}{\partial \kappa_i} \quad i = 2, 4, 5 \quad (100)$$

$$\frac{\partial g_2}{\partial \kappa_3} = -\frac{1}{\lambda'} \frac{\partial \Delta \varepsilon_{v,k+1}^{\text{in}}}{\partial \kappa_3} - \Delta t_{k+1} c_2 \exp [-(\alpha U_0 - \beta F_{k+1/2})/RT] \frac{U_0}{RT} \quad (101)$$

$$\frac{\partial g_2}{\partial \kappa_6} = -\frac{1}{\lambda'} \frac{\partial \Delta \varepsilon_{v,k+1}^{\text{in}}}{\partial \kappa_6} + \Delta t_{k+1} c_2 \exp [-(\alpha U_0 - \beta F_{k+1/2})/RT] \frac{F_{k+1/2}}{RT} \quad (102)$$

$$\frac{\partial g_2}{\partial \kappa_7} = -\frac{1}{\lambda'} \frac{\partial \Delta \varepsilon_{v,k+1}^{\text{in}}}{\partial \kappa_7} + \Delta t_{k+1} \exp [-(\alpha U_0 - \beta F_{k+1/2})/RT] \quad (103)$$

with

$$\frac{\partial \Delta \varepsilon_{v,k+1}^{\text{in}}}{\partial \kappa_1} = \frac{\Delta \varepsilon_{v,k+1}^{\text{in}}}{\lambda'} \quad (104)$$

$$\frac{\partial \Delta \varepsilon_{v,k+1}^{\text{in}}}{\partial \kappa_2} = \frac{1}{RT} \Delta \varepsilon_{v,k+1}^{\text{in}} (1 + 1/\kappa) \left(\coth \left(\frac{\Delta V}{RT} \sigma_{v,k+1/2} \right) \right) \sigma_{v,k+1/2} \quad (105)$$

$$\frac{\partial \Delta \varepsilon_{v,k+1}^{\text{in}}}{\partial \kappa_3} = \frac{1}{\kappa} \Delta \varepsilon_{v,k+1}^{\text{in}} \frac{U_0}{RT} \quad (106)$$

$$\frac{\partial \Delta \varepsilon_{v,k+1}^{\text{in}}}{\partial \kappa_4} = -\frac{\Delta \varepsilon_{v,k+1}^{\text{in}}}{\kappa^2} \left(\frac{U_0}{RT} (\alpha - 1) + \ln \left(2 \sinh \left(\frac{\Delta V}{RT} \sigma_{v,k+1/2} \right) \right) \right) \quad (107)$$

$$\frac{\partial \Delta \varepsilon_{v,k+1}^{\text{in}}}{\partial \kappa_5} = \frac{1}{c_1} \Delta \varepsilon_{v,k+1}^{\text{in}} \quad (108)$$

$$\frac{\partial \Delta \varepsilon_{v,k+1}^{\text{in}}}{\partial \kappa_6} = 0 \quad (109)$$

$$\frac{\partial \Delta \varepsilon_{v,k+1}^{\text{in}}}{\partial \kappa_7} = 0. \quad (110)$$

References

- [1] Barthold F J 1993 Theorie und Numerik zur Berechnung und Optimierung von Strukturen aus isotropen, hyperelastischen Materialien. *Dissertation IBNM Research Report*, University of Hannover
- [2] Bertsekas D P 1982 Projected Newton methods for optimization problems with simple constraints *SIAM J. Control Opt.* **20** 221-46
- [3] Dennis J E and Schnabel R B 1983 *Numerical Methods for Unconstrained Optimization and Non-linear Equations* (Englewood Cliffs, NJ: Prentice Hall)
- [4] Gill P E, Murray W and Wright M H 1981 *Practical Optimization* (London: Academic)
- [5] Grippo L, Lampariello F and Luicidi S 1991 A class of nonmonotone stabilization methods in unconstrained optimization *Numer. Math.* **59** 779-805
- [6] Kluge R 1985 *Zur Parameterbestimmung in nichlinearen Problemen (Teubner Texte zur Mathematik, Band 81)* (Leipzig: Teubner)
- [7] Kublik F 1991 Vergleich zweier Werkstoffmodelle bei ein- und mehrachsigen Versuchsdurchführungen im Hochtemperaturbereich *Dissertation*, University of Braunschweig
- [8] Lösche T 1985 Zur Entwicklung eines Werkstoffgesetzes für die Hochtemperaturplastizität über einen Markow-Prozess *Dissertation*, University of Braunschweig
- [9] Louis A K 1989 *Inverse und Schlecht Gestellte Probleme* (Stuttgart: Teubner)
- [10] Luenberger D G 1984 *Linear and Non-linear Programming* 2nd edn (Reading, MA: Addison-Wesley)

- [11] Mahnken R 1992 Duale Verfahren für nichtlineare Optimierungsprobleme in der Strukturmechanik *Dissertation*, Forschungs- und Seminarberichte aus dem Bereich der Mechanik der Universität Hannover, F 92/3
- [12] Powell M J D 1977 A fast algorithm for nonlinear constrained optimization calculations *Numerical Analysis; Proc. of the Biennial Conf. (Dundee, June 1977) (Springer Lecture Notes in Mathematics 630)* ed G A Watson (Berlin: Springer)
- [13] Schittkowski K 1981 The non-linear programming method of Wilson, Han and Powell with an augmented Lagrangian type line search function *Numerische Mathematik* **38** 83–114
- [14] Schwefel K P 1977 *Numerische Optimierung von Computer-Modellen mittels der Evolutionsstrategie* (Basel: Birkhäuser)
- [15] Servi I S and Grant N J 1951 *Creep and stress rupture behavior of aluminium as a function of purity* *Trans. AIME* **191** 909–16
- [16] Steck E A 1985 A stochastic model for the high-temperature plasticity of metals *Int. J. Plast.* **1** 243–58